

Article

Genetic Differentiation and Population Genetic Structure of the Chinese Endemic *Dipteronia* Oliv. Revealed by cpDNA and AFLP Data

Guoqing Bai ^{1,2}, Tao Zhou ^{1,3}, Xiao Zhang ¹, Xiaodan Chen ¹, Jia Yang ¹, Zhonghu Li ¹ and Guifang Zhao ^{1,*}

- ¹ Key Laboratory of Resource Biology and Biotechnology in Western China, Ministry of Education, College of Life Sciences, Northwest University, Xi'an 710069, China; bgq@ms.xab.ac.cn (G.B.); woody196@163.com (T.Z.); zhxiaao@163.com (X.Z.); chenxiaodan501@163.com (X.C.); yjhgxd@126.com (J.Y.); lizhonghu@nwu.edu.cn (Z.L.)
- ² Shaanxi Engineering Research Centre for Conservation and Utilization of Botanical Resources, Institute of Botany of Shaanxi Province, Xi'an 710061, China
- ³ School of Pharmacy, Xi'an Jiaotong University, Xi'an 710061, China
- * Correspondence: gfzhao@nwu.edu.cn; Tel./Fax: +86-29-88302411

Received: 2 July 2017; Accepted: 31 October 2017; Published: 6 November 2017

Abstract: *Dipteronia* Oliv. is an endangered genus found in China with two species, *D. sinensis* and *D. dyeriana*. Previous morphological, cytogenetic, and molecular studies have suggested that *D. dyeriana* is a species related to *D. sinensis*. However, it is unclear how the two species diverged and whether gene flow exists between these two species. Here, we performed a molecular study at the population level to characterize genetic differentiation and decipher the phylogeographic history for *Dipteronia* species based on newly sequenced chloroplast DNA (cpDNA) and amplified fragment length polymorphisms (AFLP) data retrieved from our previous studies. No haplotype was shared between the two species in the cpDNA network. However, the phylogenetic analysis suggested that a haplotype found in *D. sinensis* (H4) showed a closer relationship with haplotypes of *D. dyeriana*. Based on our estimated time of divergence, these two cpDNA haplotype lineages of *Dipteronia* diverged at about 31.19 Ma. Furthermore, two genetic clusters with asymmetric gene flow were supported based on the structure analysis, which corresponded with the two *Dipteronia* species, and we also detected a low level of asymmetric gene flow between these two species according to the MIGRATE analysis using AFLP data. During the Last Glacial Maximum (LGM, c.21 kya BP), the genus' predicted distribution was more or less similar to that at present, which was also supported by the mismatch analyses that showed no population expansion of the two *Dipteronia* populations after the LGM. The combined cpDNA and AFLP data revealed significant genetic differentiation between the two *Dipteronia* species with asymmetric gene flow, which can be explained by the varying phylogeographical histories of these two species.

Keywords: chloroplast DNA; AFLP; genetic structure; phylogeographic history; refugia; *D. sinensis*; *D. dyeriana*

1. Introduction

The geographical distribution of genetic variation in extant populations has generally resulted from interactions between two fundamental processes: population dynamics in response to past geological or climatic changes and a species' evolutionary ability to respond to natural selection [1]. A detailed examination of genetic variation within and between populations can help explain the phylogeographic history of a species in response to past geological and climatic oscillations. Numerous studies have

identified glacial refugia for temperate plant species and traced their postglacial recolonization routes [2–7]. The Quaternary climatic oscillations and the associated regional-scale geological events probably promoted intra-specific divergence due to the survival of populations in different glacial refugia and the subsequent barriers to dispersal during recolonization [1]. Recent genetic studies conducted in the Chinese population have confirmed the effects that the Quaternary climate oscillations had on the genetic structure of plants, such as *Juniperus przewalskii*, *Pinus tabulaeformis*, and *Rhododendron simsii* [8–11]. Climatic oscillations during the Pleistocene resulted in several glacial–interglacial cycles, which caused the expansion and contraction of habitats of, for example, *Juniperus przewalskii*, *Pinus tabulaeformis*, and *Rhododendron simsii* [4,8,9,11,12]. Although no massive ice sheets developed in Central China during glacial periods, the tremendous global climatic changes, together with local climatic changes caused by the Qinghai-Tibet Plateau uplift particularly during Quaternary glaciations, have affected the distribution and evolution of many plant species in this area [8,13]. In recent years, chloroplast DNA (cpDNA) markers have been frequently utilized to survey the population genetic structure and phylogeography of plants [14], and to locate refugia and post-glacial recolonization routes [14,15]. In addition, the bi-parentally inherited AFLP marker has also been used in genetic mapping [16], estimations of phylogenetic relationships [17], and genetic diversity studies [18].

The genus *Dipteronia* Oliv. (Aceraceae) is found in China with two extant species, *D. sinensis* Oliv. and *D. dyeriana* Henry. Both species are diploid ($2n = 18$) trees distributed in the broad-leaved deciduous forests in central and southern China, occurring along mountain streams at altitudes of 1000–2400 m above the sea level [19]. Two species are deciduous trees or small trees with a height of up to 10–25 m tall and pinnately compound leaves. Individual trees are andromonoecious, having both male and bisexual flowers that are born in paniculate inflorescences. The distinction between *D. sinensis* and *D. dyeriana* is mainly based on morphology. For example, the panicles of *D. dyeriana* are densely yellow-green pubescent, unlike in *D. sinensis*. The fruit of *D. dyeriana* is larger than the fruit of *D. sinensis* [20]. Controlled pollination tests revealed that *D. dyeriana* is self-compatible, but a high bee pollinator activity is generally observed in the field, suggesting that the species is at least partially reproduced by insect-mediated outcrossing. Similar to *Acer*, the genus *Dipteronia* has schizocarpic winged fruits (samaras) borne in pairs, but in contrast to *Acer*, the seeded mericarps or "nutlets" are winged essentially all the way around the seed. These fruits, whose broad wings turn from light green to red with ripening, are apparently dispersed by wind [21]. These two species are rare and endangered with a limited population and have been listed in Chinese Rare and Endangered Plant Species [22]. Studies have shown that rare or endangered species are essential to the conservation of biodiversity and the restoration and survival of the ecosystem [23]. Additionally, *Dipteronia* is one of the ancient relic woody genera in the floristic region of the Northern Hemisphere and the fossil record shows that species of this genus were once distributed in North America (from the late Paleocene to the early Oligocene) in the Tertiary [19,24,25]. The Quaternary glaciation has been suggested as the cause of the extinction of this genus in North America, because during the glaciation, the northern part of North America was mostly covered by continental icecaps [26,27]. In contrast, the Quaternary glaciers in China were mainly developed in a few mountains and no major icecaps formed [28,29]. Many Tertiary relic plants, such as *Dipteronia*, could survive in refugia in central and southern China, although their distribution area has been significantly fragmented by the glaciations. Thus far, most studies on *Dipteronia* have been focused on morphological development and taxonomy [30–33]. Only a few studies have been conducted to research the genetic diversity and genetic structure of *Dipteronia* [34], in which only the genetic diversity and differentiation of the two *Dipteronia* species have been described based on AFLP analysis [35].

In the present study, we integrated new cpDNA analysis and previous AFLP data [35] to infer the historical and contemporary divergence, in addition to the genetic diversity, of *Dipteronia* across multiple individuals and populations covering its natural ranges in China. Specifically, we aimed to

determine the amount of sequence divergence and potential interspecific gene flow after divergence between *D. sinensis* and *D. dyeriana*, as well as to infer the possible refugia.

2. Materials and Methods

2.1. Sample Collection

In this study, 18 natural populations distributed throughout each species' range were sampled, including 15 individuals from each population (Figure 1 and Table 1). Individuals of the sampled populations were separated by at least 10 m. In addition, using a closely related species, five *Acer miaotaiense* P. C. Tsong individuals were selected as an outgroup. Young leaves were collected, dried in a plastic bag with silica gel, transported to the laboratory, and stored in a $-80\text{ }^{\circ}\text{C}$ freezer until DNA extraction.

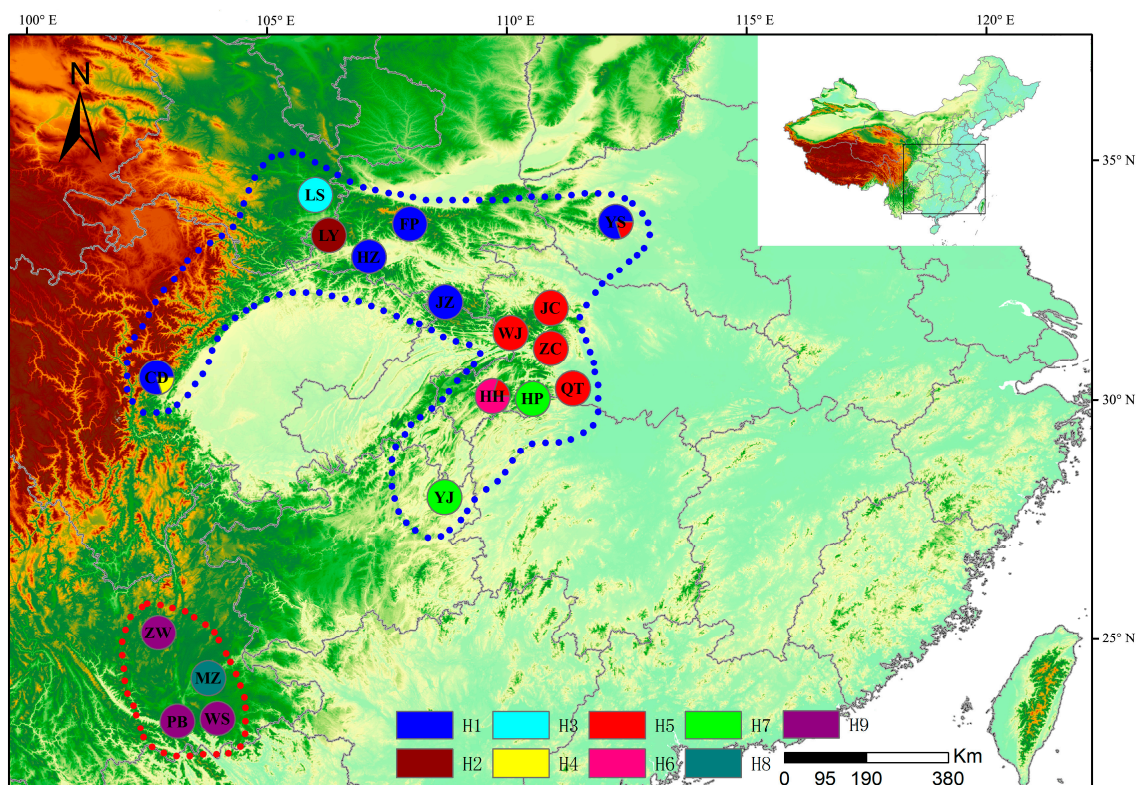


Figure 1. The distribution of nine chloroplast DNA haplotypes identified within 18 *Dipteronia* Oliv. Haplotype colors corresponds to those in Figure 2. The blue and red dotted areas represent the distribution areas of *D. sinensis* and *D. dyeriana*, respectively. Population abbreviations correspond to those given in Table 1.

Table 1. Details of sample locations (taken from GPS coordinates), sample sizes, and chloroplast DNA haplotype frequencies for 18 populations of *Dipteronia* Oliv. in China.

Code	Sample Location	Latitude	Longitude	Altitude (m)	Number	Haplotype (Sample Number)
<i>D. sinensis</i>						
FP	Fo-ping	33°40'	107°41'	1154	15	H1 (15)
HZ	Han-zhong	32°08'	105°30'	1603	15	H1 (15)
LY	Lue-yang	33°35'	106°16'	1346	15	H2 (15)
LS	Long-shan	34°21'	106°00'	1526	15	H3 (15)
CD	Chuan-dongzi	30°28'	102°42'	1468	15	H1 (12), H4 (3)
JZ	Jian-zhu	32°03'	108°43'	1479	15	H1 (15)

Table 1. Cont.

Code	Sample Location	Latitude	Longitude	Altitude (m)	Number	Haplotype (Sample Number)
YS	Yao-shan	33°43'	112°16'	1138	15	H1 (12), H5 (3)
HH	Hou-he	31°19'	110°29'	1297	15	H5 (3), H6 (12)
JC	Jiu-chongshan	31°24'	110°33'	870	15	H5 (15)
QT	Qing-tanwan	31°03'	110°55'	1685	15	H5 (15)
WJ	Wan-jiagou	31°24'	110°33'	811	15	H5 (15)
ZC	Zhu-caogou	31°05'	110°55'	1735	15	H5 (15)
HP	Hu-pingshan	30°01'	110°31'	1500	15	H7 (15)
YJ	Yin-jiang	27°59'	108°42'	1098	15	H7 (15)
<i>D. dyeriana</i>						
MZ	Meng-zi	23°24'	103°23'	1902	15	H8 (15)
PB	Ping-bian	23°01'	103°52'	2019	15	H9 (15)
WS	Wen-shan	23°37'	104°24'	2217	15	H9 (15)
ZW	Zhi-wuyuan	25°02'	102°54'	1923	15	H9 (15)

2.2. DNA Extraction and PCR Amplification

Total genomic DNA was extracted from dry leaves using a modified CTAB method [36,37], before being kept at $-20\text{ }^{\circ}\text{C}$ for long-term storage or $4\text{ }^{\circ}\text{C}$ for immediate use. The initial screening of eight cpDNA markers using a subset of 30 samples from five populations revealed four cpDNA markers (*trnV* intron, *rps18-rpl20*, *rpl20-rps12*, and *trnH-psbA*), generating genetic variations that were used for subsequent phylogeographical analyses (Table 2).

Table 2. Characteristics of the four chloroplast DNA spacer regions of *Dipteronia* Oliv.

Region	Size Range (bp)	Total Number of Mutations	N° Polymorphic Sites	Parsimony Informative Sites (Two Variants)
<i>trnV</i> intron	408	6	6	6
<i>rps18-rpl20</i>	415 (404–415)	6	6	6
<i>rpl20-rps12</i>	560 (559–560)	10	10	10
<i>trnH-psbA</i>	356 (356–399)	15	14	14

Amplification reactions (50 μL) contained 2.0 mM MgCl_2 , 0.25 mM dNTPs, 50–100 ng DNA, 0.8 mM of each primer, $1 \times$ PCR Buffer, and 2 U Taq DNA polymerase. Amplifications were conducted using the following cycling profile: $94\text{ }^{\circ}\text{C}$ for 5 min, 30 cycles of $94\text{ }^{\circ}\text{C}$ for 45 s, $53\text{--}60\text{ }^{\circ}\text{C}$ for 55 s, $72\text{ }^{\circ}\text{C}$ for 1 min, and $72\text{ }^{\circ}\text{C}$ for 7 min. All PCR products were purified from agarose gels using a PCR Product Purification Kit (Shanghai Sangon Biological Engineering Technology & Service Co., Ltd., Shanghai, China) and were sequenced in both directions by standard methods on an ABI 377 automated sequencer in Shanghai Sangon Biological Engineering Technology & Service Co., Ltd.

2.3. Data Analysis

2.3.1. Chloroplast Data Analysis

Multiple alignments of the cpDNA sequences were manually performed using ClustalX v1.83 [38] and BioEdit v7.0.4.1 [39]. Insertions/deletions (indels) were generally retained so as to increase the number of matching nucleotides in a sequence position. Nucleotide diversity (π) and haplotype diversity (H_d) [40] among the population were calculated using the DnaSP v5.0 [41]. Neutrality tests, such as Tajima's D and Fu's F_s , were also calculated with this program. We also calculated within-population diversity (H_S), total diversity (H_T), and population differentiation (G_{ST}) at the species level. To incorporate the relationships between haplotypes, an estimate of population subdivision for phylogenetically ordered alleles (N_{ST}) was obtained. A higher N_{ST} than G_{ST} usually indicates the presence of a phylogeographic structure. All aforementioned parameters were calculated

using the program HAPLONST [42]. A statistical parsimony haplotype network based on the matrix of pairwise differences between haplotypes was obtained with the aid of the TCS 1.06 [43] using the 95% connection probability limit, treating gaps as single evolutionary events. To investigate genetic differentiations between two species and among each species, the analysis of molecular variance (AMOVA) was performed with the program ARLEQUIN ver. 3.5 [44], while the significance of variance components was tested with 10,000 permutations. Mismatch distribution analyses were carried out in ARLEQUIN ver. 3.5 [44] to infer the historical demographic expansion events within the two species.

The best fitted model of DNA substitutions (HKY + I) was selected using the Akaike information criterion (AIC) method in Modeltest v2.3 [45]. The Bayesian Markov Chain Monte Carlo (BMCMC) phylogenetic estimate was inferred using MrBayes v3.1.2 [46] with default priors. *Acer miaotaiense*, which is closely related to *Dipteronia* [47], was used as an outgroup for creating the root of the Bayesian tree. Bayesian analysis was performed with 20,000,000 generations. Four simultaneous chains were run by sampling every 1000 generations. The first 25% of the total trees were discarded and >50% posterior probability consensus trees from the remaining trees were calculated and combined to a final tree. The divergence times for different *Dipteronia* cpDNA haplotype lineages were estimated using a Bayesian approach implemented in BEAST v1.5.4 [48] using the HKY + I model. The starting tree was randomly generated. We chose a coalescent tree model, which assumed a constant size for our tree. The mean cpDNA mutation rate reported in a previous study for *Acer mono* [49] was used for the four concatenated cpDNA non-coding regions to estimate the lineage divergent time in BEAST under the uncorrelated lognormal clock model. Three separate MCMC analyses were run for 20,000,000 generations with sampling at every 2000 generations and the first 25% generations were discarded as 'burn-in'. Tracer v1.5 [50] was used to check the parameters and ensure that all the effective sample size (ESS) values were greater than 200. The final tree was generated using the TreeAnnotator v1.8.2 program and visualized in FigTree v1.4.2.

2.3.2. Analysis of AFLP Datasets

We re-scored and re-analyzed two available AFLP datasets: one mainly contained populations of *D. sinensis* Oliv. (121 individuals), while the other mainly contained populations of *D. dyeriana* Henry (21 individuals) [35]. These datasets were initially generated and analyzed as part of several larger meta-studies [35]. The population structure was detected using the model-based Bayesian algorithm in STRUCTURE v2.3.4 [51]. We used the admixture model without prior information on population membership and assumed independent allele frequencies among populations. The number of clusters (K) was set to vary depending on the data set. For each value of K, we conducted 10 independent simulations with a burn-in and run length of 100,000 Markov chain Monte Carlo (MCMC) replications. The number of gene pools was inferred by estimating ΔK and $\ln P(D)$ [51–53].

The historical gene flow between *D. sinensis* and *D. dyeriana* was estimated using MIGRATE v3.1.3 [54]. The MIGRATE program calculates maximum likelihood (ML) estimates for both migration rates and effective population size between pairs of populations using a coalescent approach [55]. We relied on a maximum likelihood estimation, using 10 short chains (10,000 trees) and three long chains (1,000,000) with 10,000 trees discarded as initial 'burn-in'. The following input was used: replicates = YES:5, randomtree = YES and heating = ADAPTIVE: 1{1 1.2 1.5 3.0} [56].

2.3.3. Species Distribution Models

Species distribution models (SDMs) were carried out in MAXENT v3.3.1 [57] to predict suitable climate envelopes for *D. sinensis* at present and during the Last Glacial Maximum (LGM: c. 21 kya before present; BP), respectively. In addition to the distribution records in this study (see Table 1), 125 collection records were obtained from the Chinese Virtual Herbarium (<http://www.cvh.org.cn>) [58] and the National Specimen Information Infrastructure of China (<http://www.nsii.org.cn>) [59]. Based on this total of 145 records, a current distribution model was developed using six bioclimatic data layers

(annual mean temperature, annual precipitation, precipitation of wettest, driest, warmest and coldest quarter) available from the WorldClim database (<http://www.worldclim.org>) [60,61] at a 2.5-arcmin resolution for the present (1950–2000). This restricted bioclimatic dataset avoided including highly correlated variables (data not shown) and thus, prevented potential overfitting [62]. This model was then projected onto the paleoclimatic dataset simulated by the COMMUNITY CLIMATE SYSTEM MODEL (CCSM v3.0; <http://pmip2.lsce.ipsl.fr/>) [63,64] to infer the extent of suitable habitats during the LGM. Preparation of the LGM palaeoclimate layers at a 2.5 arc-min resolution used the same method as a previous study [65]. The accuracy of each model prediction was tested by calculating the area under the ROC Curve (AUC) [66], while AUC values > 0.8 indicate accurate simulations for the SDM models.

3. Results

3.1. Chloroplast DNA Polymorphism

In this study, the total alignment length of four regions (*trnV* intron, *rps18-rpl20*, *rpl20-rps12*, and *trnH-psbA*) was 1789 bp. A total of nine haplotypes were identified based on the total alignment sequence (Figure 1, Tables 1 and 2). There are seven haplotypes in *D. sinensis* and two haplotypes in *D. dyeriana*, with no shared haplotype between them. The distribution of nine haplotypes was shown in Figure 1 and the most widespread haplotypes were H1 (in five populations), H5 (in six populations), and H9 (in three populations). All the remainders were unique to a specific population (Figure 1; and Table 1). There were three populations that harbored two haplotypes, while the remaining populations only contained a single cpDNA haplotype (Figure 1; and Table 1). The unrooted network of *Dipteronia* Oliv. haplotypes was broadly consistent with the strict consensus tree with a star-like genealogical signature. The ancestral-like haplotype H5 lies at the center with other derivative haplotypes connected to it independently. H4 was a haplotype of *D. sinensis*, which connected to H9 of *D. dyeriana* (Figure 2). In the phylogeny tree, H4 haplotype belonged to *D. yeriana*. It was predicted that the H4 haplotype was the ancestral haplotype and became extinct in *D.yeriana* because it couldn't adapt to the environment. However, it was still reserved in *D. sinensis*.

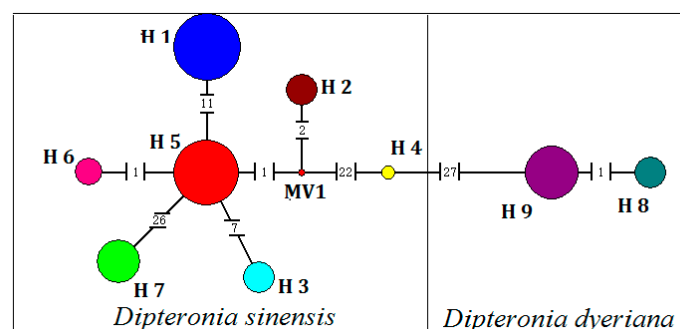


Figure 2. TCS-derived network of genealogical relationships between the nine haplotypes found in *Dipteronia* Oliv. Missing haplotypes are represented by hatch marks. The sizes of circles are approximately proportional to sample size.

3.2. Genetic Diversity and Population Differentiation

For *D. sinensis*, the cpDNA revealed a low level of haplotype diversity ($H_d = 0.260$) and nucleotide diversity ($\pi = 0.63 \times 10^{-3}$). The analysis of genetic diversity in the *D. sinensis* population showed that the total genetic diversity ($H_T = 0.812$) was much higher than the average within-population diversity ($H_S = 0.086$) (Table 3). Additionally, the G_{ST} and N_{ST} values were 0.894 and 0.912, respectively. A statistical analysis using a permutation test showed that the N_{ST} value was higher than the G_{ST} value ($p > 0.05$), indicating an absence of phylogeographical structure for *D. sinensis*. With respect to *D. dyeriana*, a lower haplotype diversity ($H_d = 0.395$) and nucleotide diversity ($\pi = 0.23 \times 10^{-3}$) was detected and the total genetic diversity ($H_T = 0.500$) was also much higher than the average

within-population diversity ($H_S = 0$) (Table 3). The AMOVA results indicated that 29.92% of the total genetic variation was partitioned between the two species, while 63.78% was found among populations (Table 4). The AMOVA analyses revealed that 67.86% and 100% of the species' total cpDNA variation was distributed among the population for *D. sinensis* ($F_{ST} = 0.89448$, $p < 0.001$) and *D. dyeriana* ($F_{ST} = 1$, $p < 0.001$), respectively, and low genetic differentiation was found within populations (Table 4).

Table 3. Genetic diversity, differentiation parameters, and neutrality test in all populations of *D. sinensis* and *D. dyeriana*.

Species	$\pi \times 10^{-3}$	H_d	H_T	H_S	G_{ST}	N_{ST}	Fu's F_s (p -Value)	Tajima's D (p -Value)
<i>D. sinensis</i>	0.63	0.260	0.812	0.086	0.894	0.912	19.053 ($p = 0.998$)	-2.365 ($p = 0.000$)
<i>D. dyeriana</i>	0.23	0.395	0.500	0	1	1	0.976 ($p = 0.534$)	0.723 ($p = 0.851$)

π = nucleotide diversity; H_d = haplotype diversity; H_T = total diversity; H_S = within-population diversity; G_{ST} = population differentiation; N_{ST} = population subdivision for phylogenetically ordered alleles.

Table 4. Different hierarchical types of analysis of molecular variance (AMOVA) of *D. sinensis* and *D. dyeriana*.

Markers	Source of Variation	df	Sum of Squares	Variance Components	Percentage of Variation (%)	Fixation Index
	Between species	1	6.734	0.160 Va	29.92	F_{CT} : 0.299
	Among populations within species	16	27.921	0.342 Vb	63.87	F_{SC} : 0.911
	Within populations	72	2.400	0.033 Vc	6.22	F_{ST} : 0.938 **
	Total	89	37.056	0.536		
<i>D. sinensis</i>	Among populations	13	24.171	0.363 Va	89.45	F_{ST} : 0.894
	Within populations	56	2.400	0.043 Vb	10.55	
	Total	69	26.571	0.406		
<i>D. dyeriana</i>	Among populations	3	3.750	0.250 Va	100	F_{ST} : 1.000
	Within populations	16	0.000	0.000 Vb	0	
	Total	19	3.750	0.250		

df = degrees of freedom; F_{CT} = correlation of chloroplast types within groups relative to the total; F_{SC} = correlation within populations relative to groups; F_{ST} = correlation within populations relative to the total; and ** $p < 0.001$.

At the species level, neutrality test statistics (Tajima's D and Fu and Li's F') (Table 3) were all non-significant, while the mismatch distributions of *D. sinensis* were multimodal (Figure 3). As the haplotypes of *D. dyeriana* contained no more than three haplotypes within the Yunnan province, the mismatch analysis was not conducted.

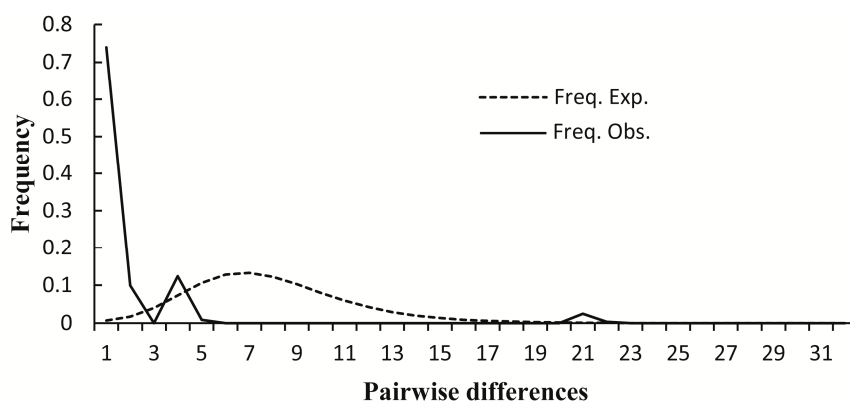


Figure 3. Mismatch distribution analysis plots for *D. sinensis*.

3.3. Phylogeny and Molecular Dating Based on cpDNA Data

In the present study, the phylogeny of cpDNA sequences was analyzed based on the Maximum likelihood (ML) and Bayes method with *Acer miaotaiense* as an outgroup (Figure 4). The phylogenetic tree derived from different methods produced an identical topology. All haplotypes were clustered into two clades with weak support values. Most haplotypes, except for one haplotype (H4), of *D. sinensis* formed a clade with a high support value, while the H4 haplotype of *D. sinensis* in the network clustered with the two haplotypes belonging to *D. dyeriana*. The BEAST-derived cpDNA chronogram indicated that the split time of the two cpDNA clades was dated to 31.2 Ma (Figure 4), with a divergence time for six haplotypes of *D. sinensis* of 7.76 Ma (95% HPD: 2.63–18.34 Ma; Figure 4) and a divergence time for two haplotypes of *D. dyeriana* of 1.04 Ma (95% HPD: 0.01–3.84 Ma; Figure 4).

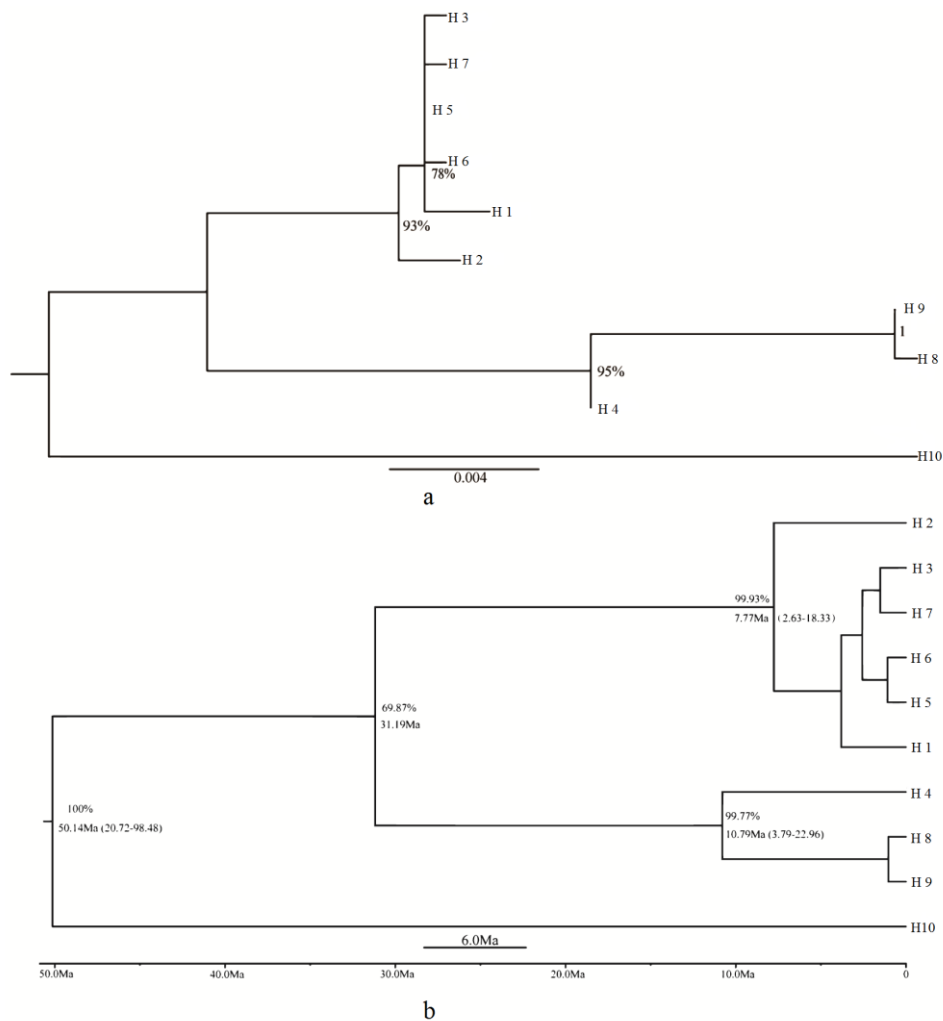


Figure 4. (a) Phylogenetic tree (ML) of the nine chloroplast haplotypes detected in *Dipteronia* Oliv. with H10 as the outgroup using *Acer miaotaiense*. (b) Beast-derived chronogram for the haplotypes in *Dipteronia* Oliv. based on four chloroplast DNA spacer regions. Posterior probabilities above 0.95 are shown above nodes. Error bars around nodes correspond to 95% highest posterior densities of divergence times. H10 marks the outgroup using *Acer miaotaiense*.

3.4. Population Structure and Interspecific Gene Flow Based on AFLP Data

In the Bayesian analysis of population structure, the highest likelihood of the AFLP data was obtained when samples were clustered into two groups ($K = 2$). All the *D. dyeriana* were clustered into groups and the populations of *D. sinensis* showed a mosaic structure, which indicated a low

level of hybridization between these two species (Figure 5). After estimating the migration rates between the two species, we detected that the mean migration rate from *D. dyeriana* to *D. sinensis* was 0.7325 (0.7054–0.7600; 95% HPD) and the reverse migration rate was 0.4860 (0.4601–0.5130; 95% HPD).

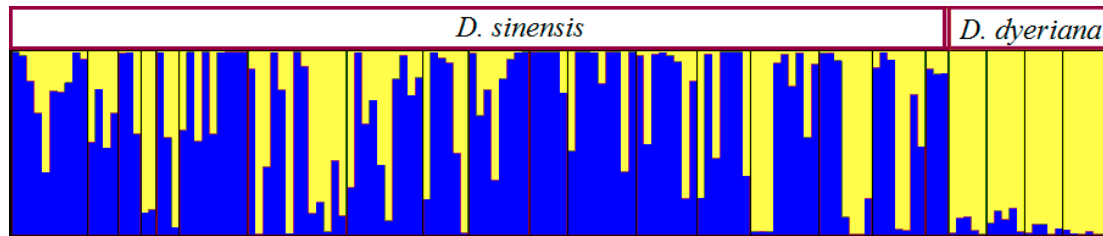


Figure 5. Clustering analysis of AFLP for *D. sinensis* and *D. dyeriana* populations using STRUCTURE.

3.5. Present and Past Ecological Niche Models

The AUC value for the current potential distribution of *D. sinensis* was relatively high (AUC > 0.9), demonstrating a reliable predictive model performance. The predicted distribution ranges of the species under the current status were identical to its actual distribution ranges (Figure 6). The actual distribution ranges of *D. dyeriana* were slightly contracted compared to the potential range during the LGM.

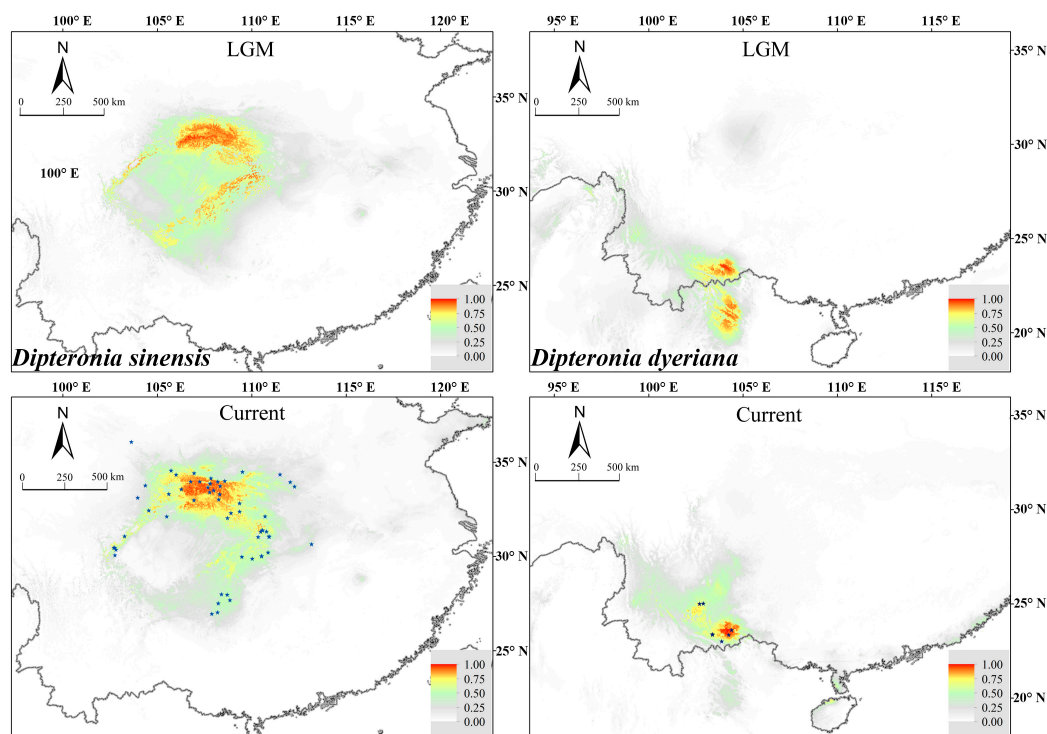


Figure 6. Potential distribution of *D. sinensis* and *D. dyeriana* based on ecological niche modeling using MAXENT; as well as the predicted distribution of the model to the last glacial maximum (c. 21 kya) and present. The color gradient from white to the red refers to habitat suitability from low to high.

4. Discussion

4.1. Genetic Diversity, Genetic Differentiation, and Glacial Refuge

The total genetic diversity of *D. sinensis* ($H_T = 0.812$) was higher than the mean total genetic diversity ($H_T = 0.670$) detected in 170 plant species for which cpDNA markers have been used [7].

The diversity was also higher compared to that of 13 other seed plants used as maternally inherited markers in China [10]. The high genetic diversity detected in *D. sinensis* might reflect the accumulation of nucleotide mutations over long evolutionary time-scales [67,68]. Previous research related to the genetic diversity of *Dipteronia* based on AFLP and random amplified polymorphic DNA (RAPD) markers also indicated that *D. sinensis* has a higher diversity [34,35]. In contrast, the genetic diversity of *D. dyeriana* found in this study was low ($H_T = 0.500$), probably due to its limited distributed area and low population sizes.

Based on our data set, high genetic differentiation was detected between these two species and variation was also detected among populations. Physical barriers may have contributed to the marked genetic differentiation among *Dipteronia* populations. Therefore, geographic isolation may also partly account for the pronounced genetic differentiation. Neighboring populations were usually separated by geographic barriers and anthropogenic facilities, which largely hindered gene flow via seed and pollen dispersal among populations. We detected high genetic differentiation and low gene flow between these two species.

According to the coalescent theory, the ancestral haplotypes are expected to occupy a central position in the network of haplotypes with a high frequency and have a great probability of producing mutational derivatives [69]. In this study, H5 was found to be predominant and geographically widespread, which was located in the interior position of genealogies (Figure 2) and is most likely the ancestral haplotype. Suitable habitats in refugia may permit species to persist for long periods. Unique genotypes and high levels of diversity often occur in these locations [2]. We inferred that the most likely refugium for *D. sinensis* was the Qinling-Daba mountains because they have the highest number of haplotypes (H1, H2, H3, and H5), as well as the highest haplotype diversity and nucleotide diversity (Figure 1 and Table 3). Meanwhile, H2 and H3 were specific to LY and LS, which were located in the Qinling mountains. The CD population had a high nucleotide and haplotype diversity, with the specific haplotype H4 belonging to it. This population was located in the west of the Sichuan basin, where there seems to be another potential refugium. The population in the Sichuan basin is surrounded by mountains of Northwest China with no glaciers in the Quaternary glacial. Compared with the same latitude, the significantly higher average temperature of the basin provides a good refuge for the genus *Dipteronia* Oliv. (Aceraceae). Additionally, the ecological niche modelling (ENM) analyses also indicated that these regions were suitable distribution ranges for these species, which also confirmed these refugia.

4.2. Demographic History of *Dipteronia*

Our phylogenetic and phylogeographic analyses based on cytoplasmic and nuclear (AFLP) data clearly support the monophyly of the genus *Dipteronia* and provide evidence for the genetic distinctiveness of *D. sinensis* and *D. dyeriana*, although asymmetric gene flow was revealed between these two species according to the STRUCTURE and MIGRATE analyses. Based on our cpDNA chronogram, the split time of the main clades was dated to the Oligocene, which indicated a long evolutionary history and independent evolution of the two species. Our molecular dating analyses (Figure 4b) indicate that the onset of haplotype diversification in *D. sinensis* (c. 7.77 Ma, 95% HPD: 2.63–18.33 Ma) occurred midway during the Pliocene period. The diversified geological and/or climatic changes had possibly acted as an isolating barrier between regional populations and promoted the diversification of two lineages of *D. sinensis*. Furthermore, the divergence time of two *D. dyeriana* haplotypes (H8 and H9) was located in the Quaternary, which indicated that the fluctuant climatic changes promoted the diversified events of *D. dyeriana* populations. However, there is a lack of fossil records of *Dipteronia* in China. We speculate that the *Dipteronia* species may have a complex evolutionary history during the long species trajectory of this endemic genus.

In the present study, no phylogeographic structure was detected for *D. sinensis*. Additionally, no expansion was detected for these two species, which indicated stable habitats where there are some species after the LGM. The ENM results also supported a rare distribution expansion for *Dipteronia* (Figure 6).

4.3. Recommendations for Species Conservation

In our study, the presence of unique *D. sinensis* cpDNA haplotypes in two different regions suggested the existence of two separate refugia. These putative refugia have long been recognized as centers of plant diversity and endemism in subtropical China [70,71]. Our results supported the hypothesis that some parts of China have been spared from the direct impact of Pleistocene glaciations [72] and have served as potential refugia for temperate deciduous trees [73,74]. The genetic data from *D. sinensis* indicated a pattern of long-term fragmentation and refugia survival, as hypothesized by Harrison et al. [73]. Although all the *D. sinensis* populations in the two proposed glacial refugia areas are currently under legal protection as one of the most endangered plant species in China, routine practices and additional precautions for the conservation of this endangered plant are still awaiting consideration with the support of genetic information.

To preserve the total genetic diversity, in situ conservation and ex situ conservation are both necessary for this endangered genus. In the current study, each suggested glacial survival area of *D. sinensis* comprised a set of populations possessing unique haplotypes and these areas should be qualified as different “evolutionary significant units” [75], such as the populations, CD, LY, HH, and LS. These distinct units can be used as a reference source for the ex situ conservation when transplanting individuals between areas or to a new site. In ex situ conservation, samples should be collected especially from those populations harboring unique haplotypes.

Currently, there are only five natural populations of *D. dyeriana* in southeast Yunnan, and our genetic survey revealed the relatively low genetic diversity of this endangered species, as had been reported in a previous study [35]. As the genetic drift or inbreeding might have decreased the within-population gene diversity of *D. dyeriana*, we recommend recovering the genetic diversity in each population through replanting the seedlings to natural habitats to increase genetic exchange and recombination. Therefore, a broad genetic sample should be preserved by ex situ conservation programs (such as seed banks and botanic gardens). This will potentially allow future reintroductions or population reinforcements, whose success will heavily depend upon the genetic quality of the available ex situ sample [76,77].

5. Conclusions

In the current study, we performed a molecular study at the population level to characterize genetic differentiation and decipher the phylogeographic history for *Dipteronia* species based on chloroplast DNA (cpDNA) and amplified fragment length polymorphisms (AFLP) data. The genetic diversity ($H_T = 0.812$) of *D. sinensis* was higher than that of *D. dyerana* ($H_T = 0.500$). The combined cpDNA and AFLP data revealed significant genetic differentiation between the two *Dipteronia* species with asymmetric gene flow, which can be explained by the varying phylogeographical histories of these two species. Based on our estimated time of divergence, the two cpDNA haplotype lineages of *Dipteronia* diverged at about 31.19 Ma. During the Last Glacial Maximum (LGM, c.21 kya BP), the genus' predicted distribution was more or less similar to that at present, which was also supported by the mismatch analyses that showed no population expansion of the two *Dipteronia* populations after the LGM.

Acknowledgments: We are grateful to Peng Zhao and Li Feng (College of Life Sciences, Northwest University, Xi'an, China) for the insightful comments and assistance. This study was co-supported by the National Natural Science Foundation of China (Grand No. 31470311, 31770229) and the Ph.D. Programs Foundation of Ministry of Education of China (Grand No. 20136101130001).

Author Contributions: Guifang Zhao and Guoqing Bai conceived and designed the experiments. Guoqing Bai, Tao Zhou and Xiao Zhang performed the experiments. Guoqing Bai, Xiaodan Chen, Jia Yang and Zhonghu Li analyzed the data. Guoqing Bai wrote the paper. All authors read and approved the final manuscript.

Conflicts of Interest: The authors declare no conflict of interest.

References

1. Avise, J.C. *Molecular Markers, Natural History, and Evolution*, 2nd ed.; Sinauer Associates, Inc.: Sunderland, MA, USA, 2004; p. 684.
2. Hewitt, G. The genetic legacy of the Quaternary ice ages. *Nature* **2000**, *405*, 907. [[CrossRef](#)] [[PubMed](#)]
3. Abbott, R.J.; Smith, L.C.; Milne, R.I.; Crawford, R.M.; Wolff, K.; Balfour, J. Molecular analysis of plant migration and refugia in the Arctic. *Science* **2000**, *289*, 1343–1346. [[CrossRef](#)] [[PubMed](#)]
4. Abbott, R.J.; Brochmann, C. History and evolution of the arctic flora: In the footsteps of Eric Hultén. *Mol. Ecol.* **2003**, *12*, 299–313. [[CrossRef](#)] [[PubMed](#)]
5. Kropf, M.; Kadereit, J.W.; Comes, H.P. Differential cycles of range contraction and expansion in European high mountain plants during the Late Quaternary: Insights from *Pritzelago alpina* (L.) O. Kuntze (Brassicaceae). *Mol. Ecol.* **2003**, *12*, 931–949. [[CrossRef](#)] [[PubMed](#)]
6. Petit, R.J.; Aguinagalde, I.; de Beaulieu, J.L.; Bittkau, C.; Brewer, S.; Cheddadi, R.; Ennos, R.; Fineschi, S.; Grivet, D.; Lasscoux, M.; et al. Glacial refugia: Hotspots but not melting pots of genetic diversity. *Science* **2003**, *300*, 1563–1565. [[CrossRef](#)] [[PubMed](#)]
7. Petit, R.J.; Duminil, J.; Fineschi, S.; Hampe, A.; Salvoni, D.; Vendramin, G.G. Comparative organization of chloroplast, mitochondrial and nuclear diversity in plant populations. *Mol. Ecol.* **2005**, *14*, 689–701. [[CrossRef](#)] [[PubMed](#)]
8. Zhang, Q.; Chiang, T.Y.; George, M.; Liu, J.Q.; Abbott, R.J. Phylogeography of the Qinghai-Tibetan Plateau endemic *Juniperus przewalskii* (Cupressaceae) inferred from chloroplast DNA sequence variation. *Mol. Ecol.* **2005**, *14*, 3513–3524. [[CrossRef](#)] [[PubMed](#)]
9. Chen, K.M.; Abbott, R.J.; Milne, R.I.; Tian, X.M.; Liu, J.Q. Phylogeography of *Pinus tabulaeformis* Carr (Pinaceae): A dominant species of coniferous forest in northern China. *Mol. Ecol.* **2008**, *17*, 4276–4288. [[CrossRef](#)] [[PubMed](#)]
10. Qiu, Y.X.; Fu, C.X.; Comes, H.P. Plant molecular phylogeography in China adjacent regions, Tracing the genetic imprints of Quaternary climate and environmental change in the world's most diverse temperate flora. *Mol. Phylogenet. Evol.* **2011**, *59*, 225–244. [[CrossRef](#)] [[PubMed](#)]
11. Li, Y.; Yan, H.F.; Ge, X.J. Phylogeographic analysis and environmental niche modeling of widespread shrub *Rhododendron simsii* in China reveals multiple glacial refugia during the last glacial maximum. *J. Syst. Evol.* **2012**, *50*, 362–373. [[CrossRef](#)]
12. Hewitt, G.M. Genetic consequences of climatic oscillations in the Quaternary. *Philos. Trans. R. Soc. Lond. B Biol. Sci.* **2004**, *359*, 183–195. [[CrossRef](#)] [[PubMed](#)]
13. Wang, H.W.; Ge, S. Phylogeography of the endangered *Cathaya argyrophylla* (Pinaceae) inferred from sequence variation of mitochondrial and nuclear DNA. *Mol. Ecol.* **2006**, *15*, 4109–4122. [[CrossRef](#)] [[PubMed](#)]
14. Ikeda, H.; Setoguchi, H. Phylogeography and refugia of the Japanese endemic alpine plant, *Phyllodoce nipponica* Makino (Ericaceae). *J. Biogeogr.* **2007**, *34*, 169–174. [[CrossRef](#)]
15. Heuertz, M.; Fineschi, S.; Anzidei, M.; Pastorelli, R.; Salvini, D.; Paule, L.; Rascaria-Lacoste, N.; Hardy, O.J.; Vekemans, X.; Vendramin, G.G. Chloroplast DNA variation and postglacial recolonization of common ash (*Fraxinus excelsior* L.) in Europe. *Mol. Ecol.* **2004**, *13*, 3437–3452. [[CrossRef](#)] [[PubMed](#)]
16. Waugh, R.; Bonar, N.; Baird, E.; Thomas, B.; Graner, A.; Hayes, P.; Powell, W. Homology of AFLP products in three mapping populations of barley. *Mo. Genet. Genomics* **1997**, *255*, 311–321.
17. Schut, J.W.; Qi, X.; Stam, P. Association between relationship measures based on AFLP markers, pedigree data and morphological traits in barley. *Theor. Appl. Genet.* **1997**, *95*, 1161–1168. [[CrossRef](#)]
18. Yuan, L.X.; Fu, J.H.; Warburton, M.; Li, X.H.; Zhang, S.H. Comparison of genetic diversity among maize inbred lines based on RFLPs, SSRs, AFLPs and RAPDs. *Acta Gene Sin* **2000**, *27*, 725–733.
19. Amy, M.M.; Steven, R.M. *Dipteronia* (Sapindaceae) from the tertiary of North America and implications for the phytogeographic history of the Aceroideae. *Am. J. Bot.* **2001**, *88*, 1316–1325.
20. Ying, J.S.; Zhang, Y.L. *Endemic Genera of Chinese Seed Plants*; Science Press: Beijing, China, 1994; pp. 57–59.
21. Tian, X.; Xu, T.Z.; Li, D.Z. New data of some Aceraceae plants in Yunnan, China. *Acta Bot. Yunnanica* **2001**, *23*, 291–292.
22. Wang, S.; Xie, Y. *China Species Red List*; Science Press: Beijing, China, 2004; p. 357.

23. Chen, C.; Lu, R.S.; Zhu, S.S.; Tamaki, L.; Qiu, Y.X. Population structure and historical demography of *Dipteronia dyeriana* (Sapindaceae), an extremely narrow palaeoendemic plant from China: Implications for conservation in a biodiversity hot spot. *Heredity* **2017**, *119*, 95–106. [[CrossRef](#)] [[PubMed](#)]
24. The Writing Group of Cenozoic Plants of China (WG CPC). *Cenozoic Plants from China, Fossil Plants of China*; Science Press: Beijing, China, 1978.
25. Manchester, S.R. Biogeographical relationships of North American Tertiary floras. *Ann. Mo. Bot. Gard.* **1999**, *86*, 472–522. [[CrossRef](#)]
26. Liu, D.S. *Quaternary Environment*; Science Press: Beijing, China, 1997; pp. 14–38.
27. Xia, Z.K. *Quaternary Environmental Science*; Beijing University Press: Beijing, China, 1997; pp. 105–118.
28. Li, S.G. *Quaternary Glaciation of China*; Science Press: Beijing, China, 1975; pp. 118–120.
29. Li, W.Q. *The Chinese Quaternary Vegetation and Environment*; Science Press: Beijing, China, 1998; pp. 183–210.
30. Zhao, X.G.; Xiao, L.; Mao, F.C. Pollen morphology of Aceraceae. *Acta Bot. Boreal.-Occident. Sin.* **1998**, *18*, 252–255.
31. Tian, X.; Jin, Q.J.; Li, D.Z. Pollen morphology of Aceraceae and its systematic implication. *Acta Bot. Yunnanica* **2001**, *23*, 457–465.
32. Qi, Y.Z.; Du, Y.J.; Li, L.M. The rare and endangered plants of Shaanxi Province for ex situ conservation in Xi'an Botanical Garden. *J. Northwest For. Coll.* **2001**, *16*, 33–36.
33. Li, S.; Cai, Y.L.; Xu, L.; Zhao, G.F. Morphological differentiation of samaras and seeds of *Dipteronia dyeriana*, Aceraceae. *Acta Bot. Yunnanica* **2003**, *25*, 589–595.
34. Li, S.; Qian, Z.Q.; Cai, Y.L.; Zhao, G.F. A comparative study on the genetic diversity of *Dipteronia sinensis* and *Dipteronia dyeriana*. *Acta Phytoecol. Sin.* **2005**, *29*, 785–792.
35. Yang, J.; Qian, Z.Q.; Liu, Z.L.; Li, S.; Sun, G.L.; Zhao, G.F. Genetic diversity and geographical differentiation of *Dipteronia* Oliv. (Aceraceae) endemic to China as revealed by AFLP analysis. *Biochem. Syst. Ecol.* **2007**, *35*, 593–599. [[CrossRef](#)]
36. Wang, G.L.; Fang, H.J. *Principles and Techniques of Plant Gene Engineering*; Science Press: Beijing, China, 1998; pp. 370–375.
37. Yang, J.; Li, S.; Cao, D.W.; Liu, Z.L.; Zhao, G.F. Construction and analysis of the AFLP reaction system of *Dipteronia* Oliv. *Acta Bot. Boreal.-Occident. Sin.* **2005**, *25*, 2173–2177.
38. Thompson, J.D.; Gibson, T.J.; Plewniak, F.; Jeanmougin, F.; Higgins, D.G. The ClustalX windows interface: Flexible strategies for multiple sequence alignment aided by quality analysis tools. *Nucleic Acids Res.* **1997**, *24*, 4876–4882. [[CrossRef](#)]
39. Hall, T.A. BioEdit: A user-friendly biological sequence alignment editor and analysis program for Windows 95/98/NT. *Nucleic Acids Symp. Ser.* **1999**, *41*, 95–98.
40. Nei, M. *Molecular Evolutionary Genetics*; Columbia University Press: New York, NY, USA, 1987; pp. 10–88.
41. Rozas, J.; Sánchez-DelBarrio, J.C.; Messeguer, X.; Rozas, R. DnaSP, DNA polymorphism analyses by the coalescent and other methods. *Bioinformatics* **2003**, *19*, 2496–2497. [[CrossRef](#)] [[PubMed](#)]
42. Pons, O.; Petit, R.J. Measuring and testing genetic differentiation with ordered versus unordered alleles. *Genetics* **1996**, *144*, 1237–1245. [[PubMed](#)]
43. Clement, M.; Posada, D.; Crandall, K.A. TCS: A computer program to estimate gene genealogies. *Mol. Ecol.* **2000**, *9*, 1657–1659. [[CrossRef](#)] [[PubMed](#)]
44. Excoffier, L.; Lischer, H.E. Arlequin suite ver 3.5: A new series of programs to perform population genetics analyses under Linux and Windows. *Mol. Ecol. Resour.* **2010**, *10*, 564–567. [[CrossRef](#)] [[PubMed](#)]
45. Posada, D.; Crandall, K.A. Modeltest: testing the model of DNA substitution. *Bioinformatics* **1998**, *14*, 817–818. [[CrossRef](#)] [[PubMed](#)]
46. Ronquist, F.; Huelsenbeck, J.P. MrBayes 3: Bayesian phylogenetic inference under mixed models. *Bioinformatics* **2003**, *19*, 1572–1574. [[CrossRef](#)] [[PubMed](#)]
47. Xiang, Q.Y.; Thomas, D.T.; Xiang, Q.P. Resolving and dating the phylogeny of Cornales—Effects of taxon sampling, data partitions, and fossil calibrations. *Mol. Phylogenet. Evol.* **2011**, *59*, 123–138. [[CrossRef](#)] [[PubMed](#)]
48. Drummond, A.J.; Rambaut, A. BEAST: Bayesian evolutionary analysis by sampling trees. *BMC Evol. Biol.* **2007**, *7*, 214. [[CrossRef](#)] [[PubMed](#)]
49. Guo, X.D.; Wang, H.F.; Bao, L.; Wang, T.M.; Bai, W.N.; Ye, J.W.; Ge, J.P. Evolutionary history of a widespread tree species *Acer mono* in East Asia. *Ecol. Evol.* **2014**, *4*, 4332–4345. [[PubMed](#)]

50. Rambaut, A.; Drummond, A.J. Tracerv1.4. Available online: <http://beast.bio.ed.ac.uk/Tracer/> (accessed on 23 April 2017).
51. Pritchard, J.K.; Stephens, M.; Donnelly, P. Inference of population structure using multilocus genotype data. *Genetics* **2000**, *155*, 945–959. [[PubMed](#)]
52. Evanno, G.; Regnaut, S.; Goudet, J. Detecting the number of clusters of individuals using the software STRUCTURE: A simulation study. *Mol. Ecol.* **2005**, *14*, 2611–2620. [[CrossRef](#)] [[PubMed](#)]
53. Cao, Y.N.; Comes, H.P.; Sakaguchi, S.; Chen, L.Y.; Qiu, Y.X. Evolution of East Asia’s Arcto-Tertiary relict *Euptelea* (Eupteleaceae) shaped by Late Neogene vicariance and Quaternary climate change. *BMC Evol. Biol.* **2016**, *16*, 66. [[CrossRef](#)] [[PubMed](#)]
54. Beerli, P. Comparison of Bayesian and maximum-likelihood inference of population genetic parameters. *Bioinformatics* **2006**, *22*, 341–345. [[CrossRef](#)] [[PubMed](#)]
55. Beerli, P.; Felsenstein, J. Maximum-likelihood estimation of migration rates and effective population numbers in two populations using a coalescent approach. *Genetics* **1999**, *152*, 763–773. [[PubMed](#)]
56. Bai, W.N.; Liao, W.J.; Zhang, D.Y. Nuclear and chloroplast DNA phylogeography reveal two refuge areas with asymmetrical gene flow in a temperate walnut tree from East Asia. *New Phytol.* **2010**, *188*, 892–901. [[CrossRef](#)] [[PubMed](#)]
57. Phillips, S.J.; Anderson, R.P.; Schapire, R.E. Maximum entropy modeling of species geographic distributions. *Ecol. Model.* **2006**, *190*, 231–259. [[CrossRef](#)]
58. The Chinese Virtual Herbarium. Available online: <http://www.cvh.org.cn> (accessed on 12 June 2015).
59. The National Specimen Information Infrastructure of China. Available online: <http://www.nsi.org.cn> (accessed on 19 October 2015).
60. The WorldClim Database. Available online: <http://www.worldclim.org> (accessed on 13 January 2017).
61. Hijmans, R.J.; Cameron, S.E.; Parra, J.L.; Jones, P.G.; Jarvis, A. Very high resolution interpolate climate surfaces for global land areas. *Int. J. Climatol.* **2005**, *25*, 1965–1978. [[CrossRef](#)]
62. Peterson, A.T.; Nakazawa, Y. Environmental data sets matter in ecological niche modelling: An example with *Solenopsis invicta* and *Solenopsis richteri*. *Glob. Ecol. Biogeogr.* **2008**, *17*, 135–144. [[CrossRef](#)]
63. The Community Climate System Model. Available online: <http://pmip2.lscce.ipsl.fr/> (accessed on 27 March 2017).
64. Collins, W.D.; Bitz, C.M.; Blackmon, M.L.; Bonan, G.B.; Bretherton, C.S.; Carton, J.A.; Chang, P.; Doney, S.C.; Hack, J.J.; Henderson, T.B. The Community Climate System Model version 3 (CCSM3). *J. Clim.* **2006**, *19*, 2122–2143. [[CrossRef](#)]
65. Sakaguchi, S.; Sakurai, S.; Yamasaki, M.; Isagi, Y. How did the exposed seafloor function in postglacial northward range expansion of *Kalopanax septemlobus*? Evidence from ecological niche modelling. *Ecol. Res.* **2010**, *25*, 1183–1195. [[CrossRef](#)]
66. Fawcett, T. An introduction to ROC analysis. *Pattern Recogn. Lett.* **2006**, *27*, 861–874. [[CrossRef](#)]
67. Chiang, T.Y.; Schaal, B.A. Phylogeography of North American populations of the moss species *Hylocomium splendens*, based on the nucleotide sequence of internal transcribed spacer 2 of nuclear ribosomal DNA. *Mol. Ecol.* **1999**, *8*, 1037–1042. [[CrossRef](#)]
68. Huang, S.; Chiang, Y.C.; Schaal, B.A.; Chou, C.H.; Chiang, T.Y. Organelle DNA phylogeography of *Cycas taitungensis*, a relict species in Taiwan. *Mol. Ecol.* **2001**, *10*, 2669–2681. [[CrossRef](#)] [[PubMed](#)]
69. Crandall, K.A.; Templeton, A.R. Empirical tests of some predictions from coalescent theory with applications to intraspecific phylogeny reconstruction. *Genetics* **1993**, *134*, 959–969. [[PubMed](#)]
70. Wang, H.S. *Floristic Geography*; Science Press: Beijing, China, 1992.
71. Ying, T.S. Species diversity and distribution pattern of seed plants in China. *Biodivers. Sci.* **2001**, *9*, 393–398.
72. Axelrod, D.I.; Al-Shehba, I.; Raven, P.H. History of the modern flora of China. In *Floristic Characteristics and Diversity of East Asian Plants*; Zhang, A.L., Wu, S.G., Eds.; Springer: New York, NY, USA, 1996; pp. 43–55.
73. Harrison, S.P.; Yu, G.; Takahara, H.; Prentice, I.C. Palaeovegetation: Diversity of temperate plants in East Asia. *Nature* **2001**, *413*, 129–130. [[CrossRef](#)] [[PubMed](#)]
74. Ray, N.; Adams, J.M. A GIS-based Vegetation Map of the World at the Last Glacial Maximum (25,000–15,000 BP). *Internetarchaeology* **2001**, *11*. Available online: <http://www.ncdc.noaa.gov/> (accessed on 14 February 2017).
75. Moritz, C. Defining significant units for conservation. *Trends Ecol. Evol.* **1994**, *9*, 373–375. [[CrossRef](#)]

76. Rita, J.; Cursach, J. Creating new populations of *Apium bermejoi* (Apiaceae), a critically endangered endemic plant on Menorca (Balearic Islands). *Anales Del Jardín Botánico De Madrid* **2013**, *70*, 27–38. [[CrossRef](#)]
77. Fernández-Mazuecos, M.; Jiménez-Mejías, P.; Rotllan-Puig, X.; Vargas, P. Narrow endemics to Mediterranean islands: Moderate genetic diversity but narrow climatic niche of the ancient, critically endangered *Naufraga* (Apiaceae). *Perspect. Plant Ecol.* **2014**, *16*, 190–202. [[CrossRef](#)]



© 2017 by the authors. Licensee MDPI, Basel, Switzerland. This article is an open access article distributed under the terms and conditions of the Creative Commons Attribution (CC BY) license (<http://creativecommons.org/licenses/by/4.0/>).